Applied Surface Science 258 (2012) 7507–7514

Contents lists available at SciVerse ScienceDirect

Applied Surface Science

journal homepage: www.elsevier.com/locate/apsusc

Effect of surface oxide on the melting behavior of lead-free solder nanowires and nanorods

Fan Gao [a], Karunaharan Rajathurai [a], Qingzhou Cui [a], Guangwen Zhou [b], Irene NkengforAcha [a], Zhiyong Gu [a,*]

[a] Department of Chemical Engineering, University of Massachusetts Lowell, Lowell, MA 01854, USA
[b] Department of Mechanical Engineering, Binghamton University, State University of New York (SUNY), Binghamton, NY 13902, USA

ARTICLE INFO

Article history:
Received 21 December 2011
Received in revised form 12 March 2012
Accepted 11 April 2012
Available online 18 April 2012

Keywords:
Nanosolder
Nanowires
Surface oxide
Melting
Flux
Nanoelectronics assembly

ABSTRACT

Lead-free nanosolders have shown promise in nanowire and nanoelectronics assembly. Among various important parameters, melting is the most fundamental property affecting the assembly process. Here we report that the melting behavior of tin and tin/silver nanowires and nanorods can be significantly affected by the surface oxide of nanosolders. By controlling the nanosolder reflow atmosphere using a flux, the surface oxide of the nanowires/nanorods can be effectively removed and complete nanosolder melting can be achieved. The complete melting of the nanosolders leads to the formation of nanoscale to microscale spherical solder balls, followed by Ostwald ripening phenomenon. The contact angle of the microscale solder balls formed on Si substrate was measured by direct electron microscopic imaging. These results provide new insights into micro- and nanoscale phase transition and liquid droplet coalescence from nanowires/nanorods to spheroids, and are relevant to nanoscale assembly and smaller ball grid array formation.

© 2012 Elsevier B.V. All rights reserved.

1. Introduction

One-dimensional nanostructures, especially nanowires, have received substantial interest in recent years due to their outstanding electrical, optical, magnetic and biological properties. However, there are still several technical obstacles against fully use of the unique properties of nanowires, which hinder the fast growth and adoption of nanowire applications. Among the important issues, a common problem in nanowire assembly and integration is unreliable interconnection between nanowires and nanowires or between assembled nanowires and electrodes/contact pads; thus, the joining of nanowires has become a critical issue for nanoelectronics assembly and packaging. Various joining processes such as welding, soldering and mechanical bonding have been proposed for the formation of nanowire interconnects [1,2]. Among various techniques proposed in the past several years, nanosoldering is a unique technique gaining increasing interest. Solder materials have been widely used in electronics assembly and board level packaging. Due to the environmental and health concern of lead, the classical tin/lead (Sn/Pb) solders are being phased out and lead-free solders in the form of binary, ternary or quaternary alloys are being extensively studied as replacements. Nanowires that contain nanosolders can be used to bond various nanocomponents or integrated surfaces. Besides the intensive research on the synthesis and fabrication of nanostructured solders, including tin/silver, tin/copper and tin/silver/copper (SAC), the thermal and electrical properties of Pb-free nanosolders in both nanoparticles and nanowires are being studied and their applications are being explored [3–5].

Reflow soldering is the most common method of chip level packaging and joining electrical components to circuit board by heating the solders and adjoining surface. There are many parameters to evaluate the property and quality of solders during the reflow. Wettability is one of those important parameters which can be experimentally assessed by measuring the contact angle of wetting [6]. A good wetting result can only be achieved if the oxides of solders are completely removed. A flux, normally an inorganic or organic acid, is often used to remove the surface oxides and therefore enhance wetting by solder in the molten state. For most soldering process, the effect of fluxes on the wettability of Sn/Pb alloy over various substrates has been extensively reported; however, the melting property of lead-free solders with one-dimensional nanostructures have not been reported. Also, due to the higher surface to volume ratio of nanostructures, oxidation effect may become prevail in the reflow soldering and this issue needs to be addressed.

In this paper, we present the melting behavior of nanosolder systems (tin and tin/silver alloy nanowires/nanorods) under

* Corresponding author. Tel.: +1 978 934 3540; fax: +1 978 934 3047.
E-mail address: Zhiyong_Gu@uml.edu (Z. Gu).

0169-4332/$ – see front matter © 2012 Elsevier B.V. All rights reserved.
http://dx.doi.org/10.1016/j.apsusc.2012.04.074

Table 1
List of fluxes used in the experiment.

Flux type	Flux full name	Product name	Composition (% wt)	pH (23 °C)	Vendor
R	Rosin	Liquid flux #5 R	Rosin (50–60) Isopropyl alcohol (40–50)	3.02 ± 0.32	Indium. Corp
RMA	Rosin mild activated	Liquid flux #5 RMA	Rosin mixture (40–50) Isopropyl alcohol (30–40) Methyl ethyl ketone (10–30) Proprietary (1–2)	2.74 ± 0.38	Indium. Corp
RA	Rosin activated	Liquid flux #5 RA	Rosin flux (40–50) Isopropyl alcohol (35–40) Methyl ethyl ketone (10–20)	2.43 ± 0.29	Indium. Corp
Stay-clean	–	Stay Clean® Liquid soldering flux	Zinc chloride (<30) Ammonium chloride (5–25) Hydrochloric acid (<5)	0.29 ± 0.05	Harris Products Group

flux influence and the micron/nano-structures formed on Si substrate. We found that the flux vapor, rather than the liquid flux, can effectively remove the nanosolder surface oxide and facilitate the phase transformation and shape change of nano-solders at temperatures even below the melting point of the bulk solder materials. Under the influence of the flux vapor, an Ostwald-ripening assisted spheroid formation was observed. The micron-scale contact angle of reflowed solders was measured by direct scanning electron microscopy imaging. Finally, the effect of temperature and type of fluxes on the melting, especially the phase transition/shape change from nanowire/nanorod to spheroids was investigated.

2. Experimental

2.1. Materials and methods

Sn and Sn/Ag alloy nanowires were fabricated using polycarbonate (PC) porous membranes (Whatman) with pore size of 30 nm and 50 nm in diameter through the electrodeposition method. First, a thin layer of Ag was evaporated on one side of a commercial PC membrane by a Nano-Master NTE-3000 thermal evaporator (Nanomaster, Inc.). The silver coated side of the membrane contacted with a copper plate and restrained by a glass joint with O-ring seal. After that, the membrane was filled with tin or tin/silver electrolyte and a current was applied with 15 mA/cm^2 density by using a pontentiostat (Model 362, Princeton Applied Research). After the plating, the membrane was dissolved in dichloromethane to release the nanowires. The detailed nanowire fabrication process can be found from our previous publication [7]. Sn nanorods were synthesized by a surfactant-assisted chemical reduction method that has been developed in our group [8]. Briefly, 40 mg tin sulfate was added in 40 mL 8 mM sodium dodecyl sulfate (SDS) solution first and stirred for 10 min. Then 24 mg of sodium borohydride was added and the solution was stirred at 350 rpm at room temperature. The nanorod formed after 30 min reaction and the product was centrifuged and cleaned by DI water and ethanol for further characterization.

For a solder reflow process in electronics/microelectronics assembly, a number of factors can influence the process, including reflow profile, roughness of substrates, flux selection, quantity or volume of molten solder, reaction between the solder material and the substrate [6]. As the first attempt of studying the melting and wetting of solder nanowires and nanorods, Si wafer was chosen as a non-reactive surface to avoid the interface diffusion and reaction between the solder and substrate. Since the traditional solder paste mixed with the micron-sized solders and liquid flux (10–15 wt%) can potentially bring the difficulty in nanosolder dispersion and the surface cleaning, flux vapor was used for nanosolder reflow.

Rosin based flux, the most widely used one in electronics manufacturing, can effectively remove the oxide from metal surfaces [9,10]. There are three types of rosin based fluxes: R (rosin) is relatively low active, RA (rosin activated) is quiet strong, while RMA (rosin mild activated) is in between (see Table 1). Nowadays, the water soluble fluxes containing inorganic chemicals such as hydrochloric acid and zinc chloride have received more attention due to the easiness for cleaning; however, these types of fluxes are often more aggressive [11]. In this paper flux RMA was studied as the main focus, while the others – R, RA and water soluble flux were investigated as comparison. The rosin based fluxes were obtained from Indium Corporation of America, and the water soluble flux (also called “stay-clean” flux) was purchased from J.W. Harris Co., Inc.

The nanosolder reflow experiments were carried out in a programmable high-temperature tube furnace. The flux RMA was dropped onto a glass substrate and placed in the furnace adjacent to a Si wafer with solder nanowires/nanorods on top. Upon heating, the liquid flux was vaporized to clean up the surface oxides of the nanosolders. Nitrogen purging was used to avoid further oxidation of nanosolders during this process. The nanosolder reflow process followed the standard industrial reflow profile including preheating, thermal soak, reflow and cooling steps. The peak temperatures were controlled at 250 °C, and the time above the melting temperature of Sn (232 °C) was 5 min. Other peak temperatures were also tried, including 220 °C and 190 °C. After reflow, the rosin based flux residual on nanosolders were cleaned by iso-propanol and then dipped into 50 °C water to clean the possible salts generated during reflow, and the water soluble stay-clean flux was only cleaned by water at 50 °C for 10 min.

2.2. Materials characterization and equipments

The morphology and composition of the solder nanowires and nanorods were analyzed by a field emission scanning electron microscopy (FESEM, model JSM-7401F) which is equipped with energy dispersive X-ray spectroscopy (EDS). For oxide growth kinetic study, the tin nanowire suspensions of as-fabricated tin nanowires, nanowires stored in ethanol for one week, and nanowires stored in ethanol up to three months were dropped on three pieces of Si wafers, respectively. Then the samples were immediately loaded into the FESEM/EDS to characterize the oxide growth. The oxide thickness of nanowire and nanorod were measured by high resolution transmission electron microscopy (HRTEM) using a JEOL-2100 microscope operated at 200 kV. The pH values of different fluxes were measured three times by a Fisher Science Education pH meter and the average values were reported with standard deviation.

3. Results and discussion

3.1. Structure and composition characterization

The structure and morphology of the solder nanowires and nanorods were characterized by FESEM as shown in Fig. 1(a)–(c). The size of the nanowires can be controlled by using the template with different pore sizes. The pure Sn nanowires with 30–50 nm in diameter and 5–6 μm in length and the Sn/Ag alloy nanowires with 50–80 nm in diameter and 5–6 μm in length were shown in Fig. 1(a) and (b), respectively. Fig. 1(c) shows the SEM image of the Sn nanorods with 70–100 nm in diameter and about 300 nm in length, which were synthesized by a surfactant-assisted chemical reduction method. The elemental analysis of the pure Sn nanorods, Sn and Sn/Ag alloy nanowires was confirmed by EDS, as shown in Fig. 1(d). The pure Sn nanowires and nanorods show very similar spectra and the composition of Sn/Ag alloy nanowires was counted at 96.5:3.5 in mass ratio that is close to the eutectic ratio with a bulk melting point of 218 °C.

The surface oxidation of solders is an important issue for soldering techniques. The formation of tin oxide has been observed on exposed Sn surfaces which can affect the wetting behavior and bonding quality [12]. Many studies have been reported on the oxide thickness of micron sized solders and their effect on the melting and soldering [13,14]; however, there is few study regarding the mechanism and kinetics of tin oxide growth at nanoscale [15]. Although the oxide growth is slow at room temperature, the tin oxide shell formed can block the molten Sn from moving and hamper effective wetting, and thus leading to the soldering failure. Fig. 2 shows the TEM characterization of both the nanowires and nanorods. The inset HRTEM images in Fig. 2 indicate the surface oxidation on both the tin nanowires and nanorods. The oxide thickness of as fabricated single Sn nanowire was measured by the HRTEM imaging in Fig. 2(a), which showed a 3–4 nm amorphous oxide layer covered on single crystalline metallic Sn structure. Fig. 2(b) reveals that the Sn nanorod is also covered by a 3–4 nm thick oxide layer, similar to the Sn nanowires. It is known that the nanoscale Sn particles have high chemical activity and can be oxidized into stable SnO_2 compounds at ambient temperature [16]. The EDS result confirms the oxide outer layer, whose effect will be further discussed in the next section.

3.2. Nanosolder reflow in different environments

To evaluate the efficiency of the flux vapor, Sn nanowires reflowed at a peak temperature of 250 °C without flux was studied as a control. As shown in Fig. 3(a), the reflow without the flux leads to the formation of discontinued Sn spheres enclosed in translucent thin shells. The thin shells are probably the tin oxide that was formed during the nanowire fabrication and/or during the cleaning/storage process. To determine the surface oxide growth, the mass ratio of oxygen to tin for the nanowires was determined by EDS analysis, as shown in Fig. 4. The EDS results imply that a thin oxide layer was formed during the nanowire fabrication and cleaning processes. Within the first week, this oxide grew significantly; however, after three-month storage in ethanol, the amount of oxygen does not show more significant increase. Since the melting point of the SnO and SnO_2 are 1080 °C and 1630 °C respectively, the oxide will not melt at 250 °C and thus the oxide shell is left over. Similar phenomenon has been observed in phase-change semiconductor material GeTe nanowires, which leads to the formation of nanotubes with remaining oxide wall [17]. Fig. 3(b) is the result from nanosolder reflow in the flux vapor environment, which shows dramatic shape change (melting) compared with the reflow without using the flux. No translucent oxide thin shells were observed, and Sn nanowires transformed to spheroids with smooth surfaces. The reflowed Sn/Ag alloy nanowires in Fig. 3(c) showed similar result as pure Sn nanowires. The wetting behavior of the resulting Sn spheroids on the Si substrate was characterized by SEM imaging. The contact angle of the Sn spheroids on the Si substrate is measured to be 130° at a SEM tilting angle of 80° as shown in Fig. 3(d). This tilting angle is close to the optimum 90°, so the measured contact angle should be close to the real value. The relatively large contact angle (greater than 90°) is caused by non-wetting Si substrate because it does not react with Sn to form intermetallic layer. Due to the high ratio of Sn composed in the Sn/Ag alloy system, the contact angle of the Sn/Ag spheroids formed on the Si substrate is very similar to that of the Sn spheroids.

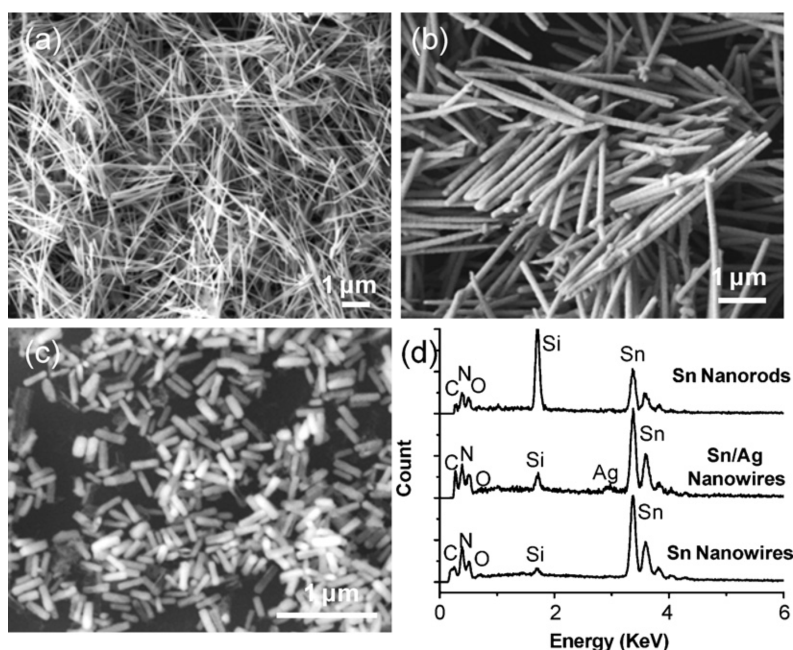

Fig. 1. Characterization of Sn and Sn/Ag alloy nanowires and nanorods. (a) SEM image of Sn nanowires; (b) SEM image of Sn/Ag alloy nanowires; (c) SEM image of Sn nanorods; (d) EDS spectra of solder nanowires and nanorods.

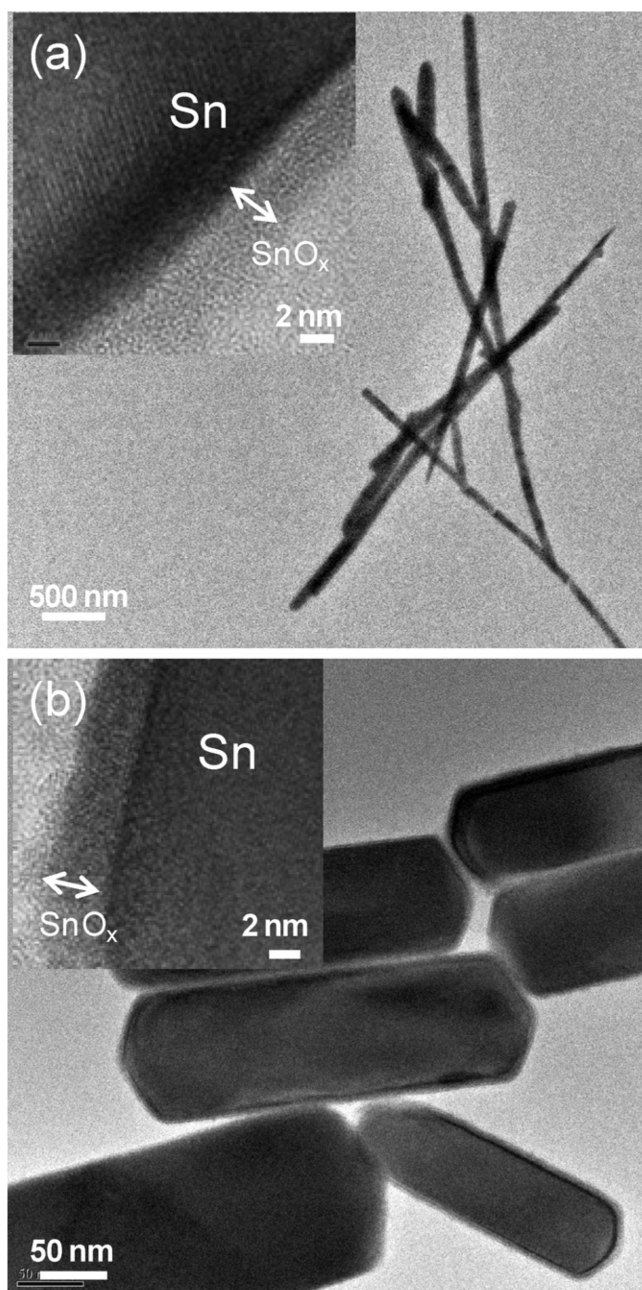

Fig. 2. TEM images of (a) Sn nanowire with a surface oxide layer; (b) Sn nanorod with a surface oxide layer. Insets are HRTEM images clearly showing two distinct regions: the Sn metal in the core of the nanowires/nanorods and the surface oxide layer.

Due to the random and non-uniform distribution of the nanowires on the Si wafer and the merging of Sn liquid droplet, the size of reflowed Sn solders varied from hundreds of nanometers to several microns, as shown in the inset SEM image in Fig. 5. The areas with more concentrated nanowires may form larger spheroids. This can be inferred from the size histogram of reflowed solder nanowires as shown in Fig. 5. Theoretically, a Sn nanowire with a typical diameter of 100 nm and length of 6 μm as shown in Fig. 1(b) can form a sphere about 0.4 μm in diameter, when assuming the same volume before and after shape change. This histogram analysis suggests that only a small portion of the nanowires was kept as single nanowires during the reflow, and most of them merged into larger spheroids and underwent an Ostwald ripening phenomenon. In order to form ordered nanosolder arrays, alignment and assembly techniques can be used to optimize the nanowire distribution and more uniform droplet/sphere formation [18].

Tin nanorods, a nanosolder system with a smaller aspect ratio, were treated by similar reflow process as well. It is shown in Fig. 6(a) that the nanorods reflowed in N_2 environment without flux had the tendency to melt and merge together. However, irregular shapes were also formed and some nanorods were still keeping the original rod shape, probably because the surface oxidation hindered the complete spheronization of the molten Sn inside the oxide shell of the nanorods. This phenomenon was similar to Sn nanowires reported in previous study [7]. Compared with the nanowires, no translucent oxidation film was observed, which may be due to the much smaller aspect ratio of nanorods. The low aspect ratio of nanorods can be approximated as zero-dimensional nanoparticle model which has been widely studied [19]. As the temperature increases beyond the melting point, the internal pressure of the liquid core increases and makes the solid oxide shell at higher tension and more easily to rapture. On the other hand, because of shorter length, the oxide shell in low aspect ratio nanorods suffers much higher tension, and hence breaks with great ease compared to the coating in nanowire with lower curvature. However, when flux was added, the oxide shell was fully removed and liquid surface tension drove the smooth spheroids formed as shown in Fig. 6(b). Compared with the nanowire reflow results, the nanorods reflowed solders have much smaller size but more uniform spheroids as shown in Fig. 6(c). The average diameter of solder balls is less than 1 μm, with a few bigger ones having a size larger than 1 μm while the smaller ones having the size less than 100 nm, around 50–60 nm. Compared with the solder nanowires, the average size of the solder balls formed from nanorods is significantly smaller than that from nanowires. This can attribute to (1) the volume of a single nanorod was smaller than a single nanowire; (2) the distribution of nanorods on the Si wafer when deposited is more uniform than that of nanowires. Nanowires obtained from the template-assisted method contain branches or bundles due to the template limitation, which make them more difficult to disperse uniformly [20], while the tin nanorods are more uniform and well dispersed.

3.3. *Temperature effect on nanosolder structure transformation*

The melting behavior of a liquid on solid is sensitive to temperature changes since a number of properties of both the liquid and the substrate can be influenced by the temperature [21]. We examined the temperature effect on Sn nanosolders with the RMA (rosin mild activated) flux at several peak temperatures: 190 °C (below the melting point, M.P.), 220 °C (close to M.P.), and 250 °C (above M.P.). Here the M.P. refers to the thermodynamic M.P. of bulk materials. The reflow time is defined as the time span during the temperature above the set temperature minus 20 °C (i.e., 170 °C, 200 °C, and 230 °C, respectively). All the reflow time was controlled in 5 min. It can be clearly seen from Fig. 7 that the melting behavior changed significantly at different reflow temperatures. Fig. 7(a) shows that at a peak temperature of 190 °C ($\sim$40 °C below the bulk M.P), a significant morphology change already occurred on Sn nanowires. The nanowires changed their wire shape to mostly round shape like and regrouped into larger clusters, suggesting that the flux was activated to remove the surface oxide and the nanowires were induced to a partial melting even at a temperature 40 °C below the M.P. For the sample treated at a peak temperature of 220 °C, the nanosolders are closer to a sphere shape and smaller clusters aggregated to form larger spheroids as shown in Fig. 7(b); however, the nanowires were still not completely reflowed yet, as shown from the non-uniform solder size and morphology. Fig. 7(c) shows the reflow result at the peak temperature of 250 °C, 20 °C above the melting point. All the nanowires completed the phase transition and

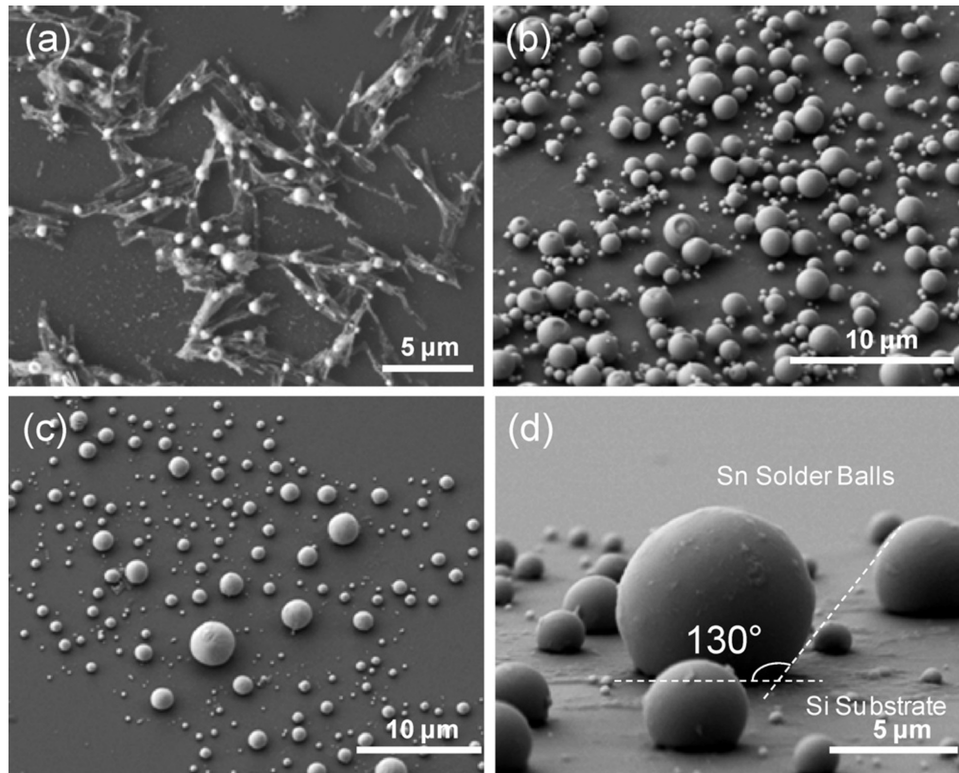

Fig. 3. SEM images of reflowed solder nanowires. (a) Sn nanowires reflowed in the N_2 environment without a flux; (b) Sn spheroids after the nanowires reflowed in the N_2 with RMA flux vapor; (c) Sn/Ag alloy nanowires reflowed in the N_2 with RMA flux vapor; (d) Microscale contact angle measurement of reflowed Sn solders on a Si wafer.

the shape changed from wires to spheroids due to the minimized surface energy at liquid phase.

Computer simulations have shown the melting point depression for Sn nanoparticles with radii ranging from 5 to 50 nm [22–24], and some previous studies for metallic nanoparticles that show a dependence of melting point on particle radius has been reported [3,25]. However, no obvious melting point depression was observed from the solder nanowires in the length of few microns in our experiments. And prior experiments indicated that there was only ~0.7 °C melting point depression from DSC measurement for these pure Sn nanowire sample [7]. It is probably due to the fact that the diameter range of the solder nanowires that we studied in this experiment did not reach significant melting point depression region. Another possible factor is the uncertainty from the melting point measurement by thermoanalytical techniques such as DSC and TGA [26]. It was found that many effects, such as particle agglomeration, surface oxidation, and size distribution, can give a large uncertainty on the melting point measurements by those thermoanalytical methods. On the other hand, it has been reported that there is a quasimelting phase distinct from the thermodynamic molten state exists in small particles where the particles are continuously fluctuating between different structures at temperature well below the melting point [27–29]. Hence, it is possible to observe the coalescence of nanowires at the temperature below the thermodynamic melting point, as long as the energy is enough to initiate the quasimelting phase. The above results that the nanowires started to melt or initiate a quasimelting process at a much lower temperature imply that the surface oxidation can significantly affect the quasimelting phase being initiated. The removal of the oxide layer and exposure of fresh metal surface

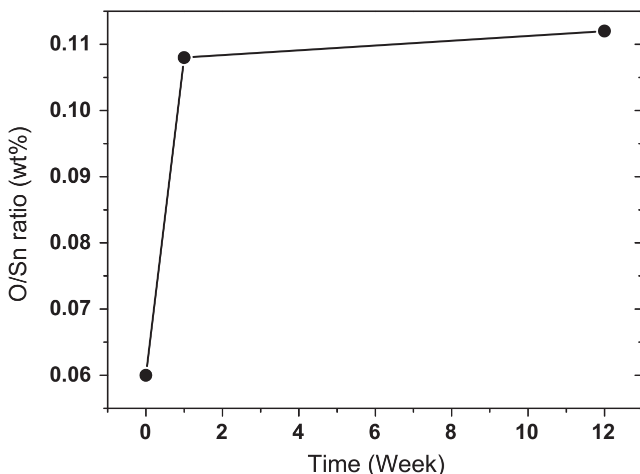

Fig. 4. The oxygen to tin mass ratio (O/Sn) characterized by EDS for nanowires stored for different time periods.

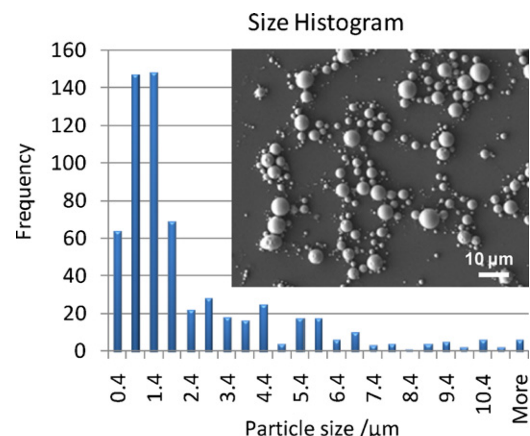

Fig. 5. SEM image and size histogram of reflowed tin (Sn) spheroids.

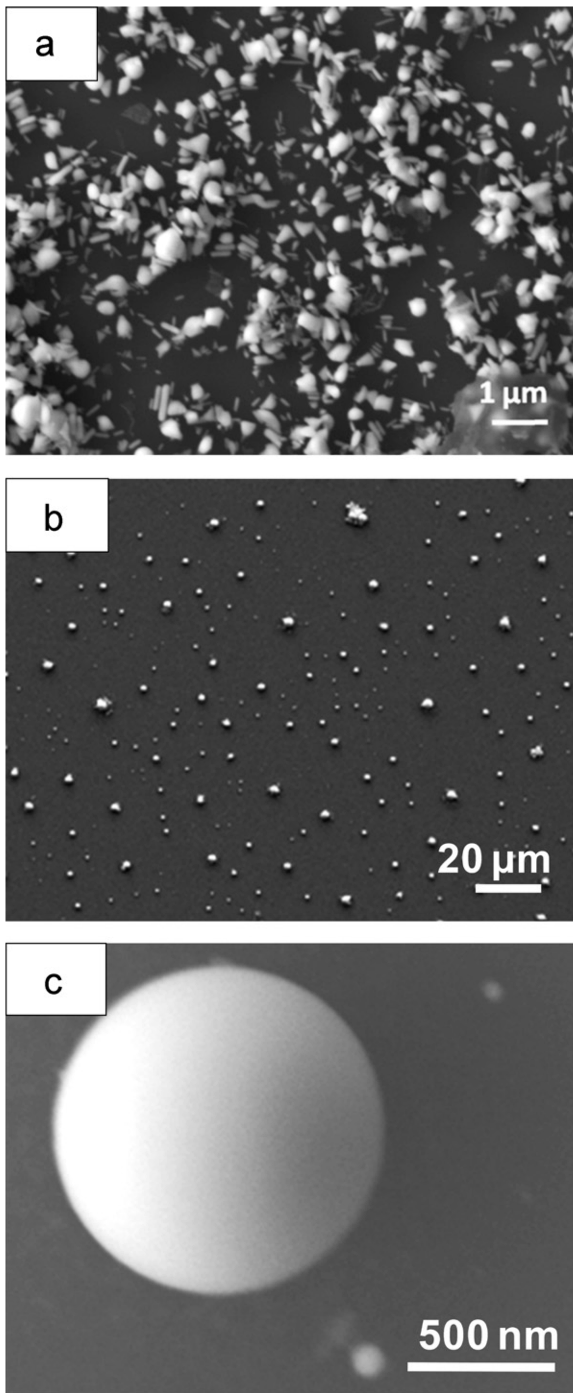

Fig. 6. Comparison of solder nanorod reflow in different environments: (a) reflowed Sn nanorods in N_2 environment (without flux vapor); (b) reflowed Sn nanorods in N_2 environment with RMA flux vapor; (c) zoom in image of nano-sized solder balls.

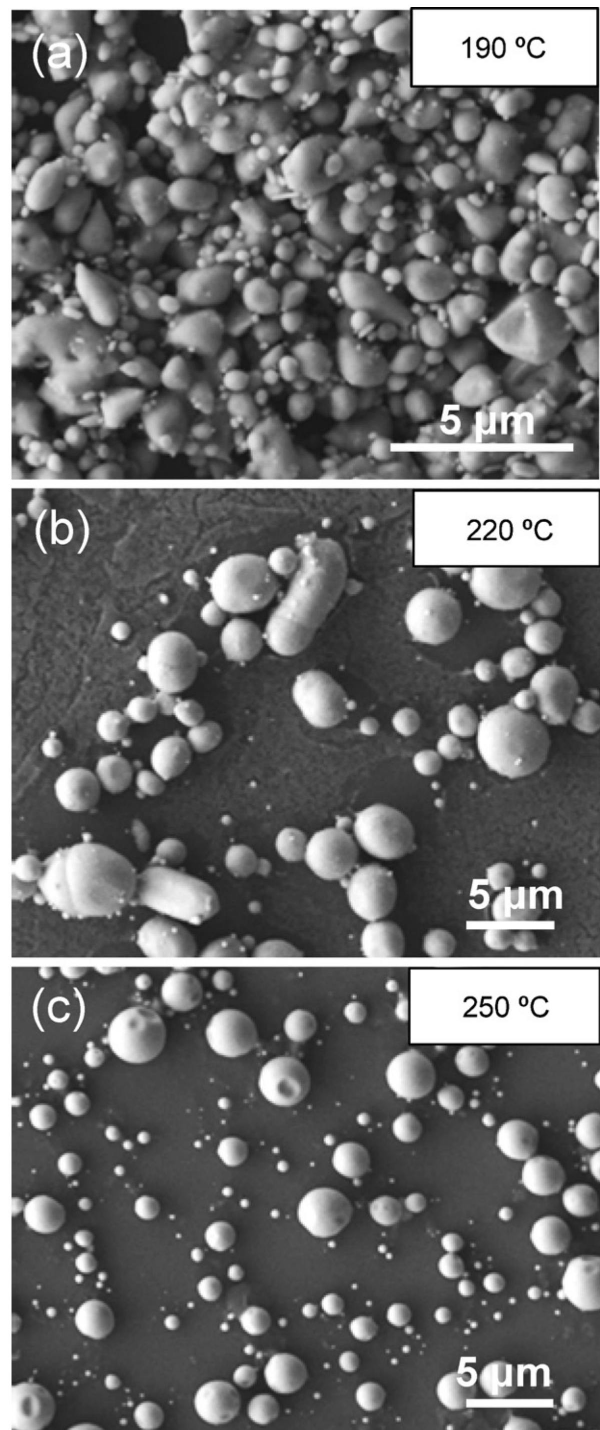

Fig. 7. Temperature effect on Sn nanowire structure transformation in N_2 environment with RMA flux vapor. The peak temperatures are (a) 190 °C; (b) 220 °C; (c) 250 °C.

helped initiate the melting process or enable a fast diffusion process so that the solder materials already have significant shape change at a relatively low temperature.

3.4. Flux effect on nanosolder structure transformation

The effect of different fluxes such as rosin based R (rosin) and RA (rosin activated), as well the stay-clean flux on Sn nanowires was compared at two different temperatures 190 °C and 250 °C, as shown in Fig. 8. Fig. 8(a), (c), (e) represents the flux R, RA and stay-clean flux vapor used in the reflow at a peak temperature of 190 °C, and Fig. 8(b), (d), (f) shows the same types of flux vapor used at a peak temperature of 250 °C, respectively. As can be seen in Fig. 8(c) and (e), spheroids formed by using flux RA and stay-clean flux showed similar trend as flux RMA at 190 °C, showing a higher activation. However, the flux R cannot be well activated at the same temperature due to its lower activation ability, and the shape change of nanowires did not take place, as noted in Fig. 8(a). The stay-clean flux is more aggressive in its ability to remove oxides, solder spheroids was formed at a peak temperature of 190 °C, about 40 °C lower than the bulk Sn melting point, as shown in Fig. 8(e).

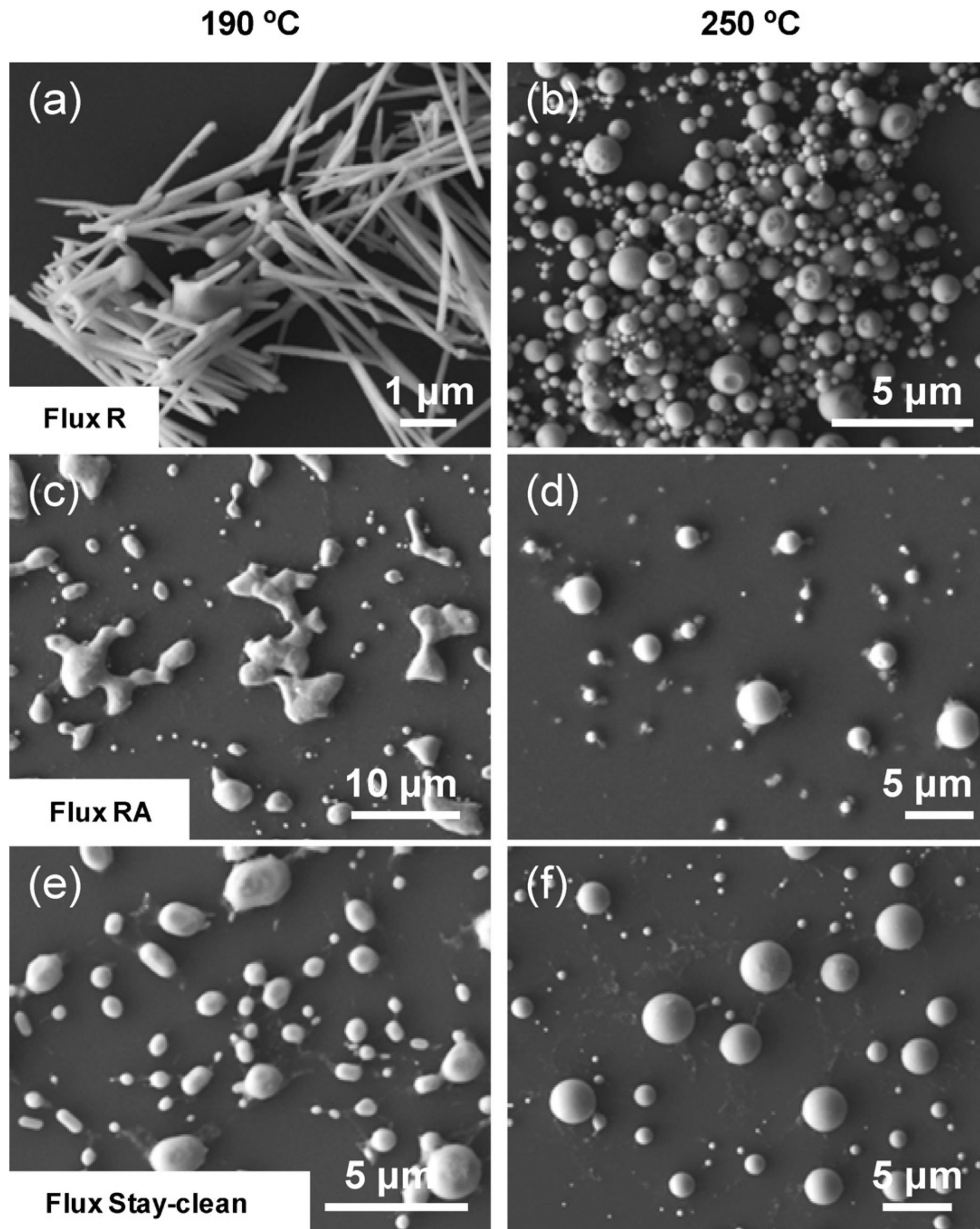

Fig. 8. Flux effect on Sn nanowire structure transformation in N_2 environment with different flux vapors at peak temperatures of 190 °C and 250 °C: (a) flux R at 190 °C; (b) flux R at 250 °C; (c) flux RA at 190 °C; (d) flux RA at 250 °C; (e) flux stay-clean at 190 °C; (f) flux stay-clean at 250 °C.

These results indicate that the acidity of the flux plays an important role in the melting of nanowires/nanorods. The flux with stronger acidity such as flux RA and stay-clean can be activated at a lower temperature and thus effectively clean the surface oxide. Although the tin nanosolder forms spheroids on the Si substrate, the reflow on the reactive surfaces such as copper, nickel or gold is expected to have more complex situation. Future study will focus on the intermetallic compound formation and growth to clarify the possible reflow temperature profile for real applications.

3.5. Ripening phenomenon

Fig. 9 shows an example presenting the thermodynamically driven ripening phenomenon which was performed by Sn nanowires reflowed in N_2 with flux R at a peak temperature of 250 °C. Different from the other fluxes, the more evidence of ripening can be obtained from the reflow process with flux R, in which the incomplete ripening process can be observed in the SEM image. Due to the relatively weaker acidity of flux R and slower cooling rate, longer time is needed to activate the flux R than the other fluxes, so the nanowires melt at a relatively higher temperature and the liquid droplets flowed slowly to merge with solders over time. When cooling started, those solders have not finished the ripening and merging process before solidification, and thus many small hemispherical solders are attached around a large one. This observed phenomenon provides important clues regarding the nanosolder growth mechanism and suggests that the detailed examination of such a mid-product of the reflow is necessary for future study of the wetting properties and mechanism of nanosolders with reactive substrates. Some uneven surfaces can be observed from most

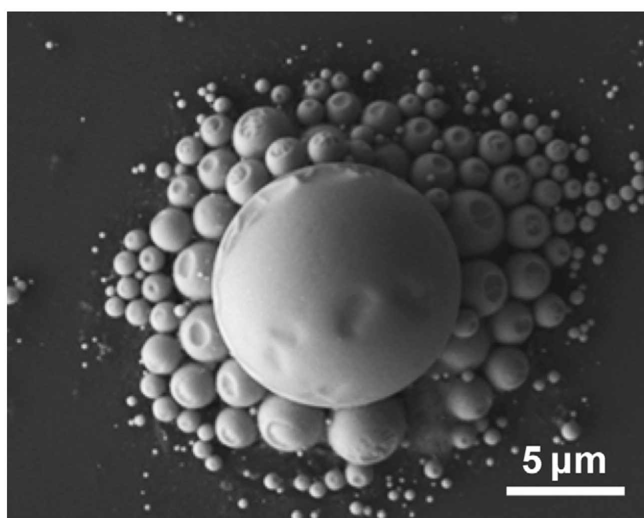

Fig. 9. SEM image showing the ripening phenomenon occurred from Sn nanowires reflowed in N_2 with flux R at a peak temperature of 250 °C.

of the reflow solders, which may be formed during the liquid solder solidification process. One possible reason is related to the liquid-to-solid shrinkage because most metals contract on freezing. Surface concave occurs as a result of the volume contraction of nanosolders during the solidification and the metal density dramatically increases. It has been reported that the uniform cooling from all sides may result in larger degree of surface shrinkage than single direction cooling from bottom of package [30]. Since the nanosolder reflow setup performed uniform cooling, it is possible to generate the uneven surfaces on reflowed nanosolder balls. Other possibilities include the N_2 flow purged though the tube, i.e., the flow of N_2 can affect the outer surface of the solders in liquid state.

4. Conclusions

In summary, it is found that the thin oxide layer on both solder nanowires and nanorods can dramatically affect the melting behavior of nanosolders. The reflow environment, especially the flux, can effectively clean the surface oxide and influence Sn and Sn/Ag alloy solder phase transition from nanowires/nanorods to spheroids. After oxide removing, micro- and nano-sized solder balls have been successfully formed from lead-free solder nanowires and nanorods with different lengths and aspect ratios. With the flux-assisted solder melting process, nanowires/nanorods may melt at a temperature below the melting point of the bulk material, which can affect potential nanosolder applications. Even though the phase transition may start to take place at a lower temperature than the melting point, a higher temperature is still important to ensure full flux activation for obtaining optimum solder reflow result. The understanding of melting and wetting of nanosolders on Si substrate help to facilitate the development of nanoscale ball grid arrays in nanoscale assembly and packaging miniaturization applications, such as MEMS/NEMS, nanosensors, and nanoelectronic devices.

Acknowledgements

Financial support from the NSF Center for High-rate Nanomanufacturing (CHN) is acknowledged. We also thank partial funding support from 3M Company (3M Non-tenured Faculty Grant).

References

[1] Y. Lu, J.Y. Huang, C. Wang, S. Sun, L. Jun, Cold welding of ultrathin gold nanowires, Nature Nanotechnology 5 (3) (2010) 218–224.
[2] Z. Gu, H. Ye, D.H. Gracias, The bonding of nanowire assemblies using adhesive and solder, JOM 57 (2005) 60–64.
[3] H. Jiang, K.-S. Moon, F. Hua, C.P. Wong, Synthesis, Thermal, Wetting properties of tin/silver alloy nanoparticles for low melting point lead-free solders, Chemistry of Materials 19 (18) (2007) 4482–4485.
[4] Q. Cui, F. Gao, S. Mukherjee, Z. Gu, Joining, Interconnect formation of nanowires and carbon nanotubes for nanoelectronics and nanosystems, Small 5 (11) (2009) 1246–1257.
[5] Z. Gu, H. Ye, D. Smirnova, D. Small, D.H. Gracias, Reflow and electrical characteristics of nanoscale solder, Small 2 (2) (2006) 225–229.
[6] G. Kumar, K.N. Prabhu, Review of non-reactive and reactive wetting of liquids on surfaces, Advances in Colloid and Interface Science 133 (2) (2007) 61–89.
[7] F. Gao, S. Mukherjee, Q. Cui, Z. Gu, Synthesis, Characterization, Synthesis, characterization, and thermal properties of nanoscale lead-free solders on multisegmented metal nanowires, The Journal of Physical Chemistry C 113 (22) (2009) 9546–9552.
[8] Q. Cui, K. Rajathurai, W. Jia, X. Li, F. Gao, Y. Lei, Z. Gu, Synthesis of single crystalline tin nanorods and their application as nano-soldering materials, The Journal of Physical Chemistry C 114 (50) (2010) 21934–21938.
[9] M. Arenas, M. He, V. Acoff, Effect of flux on the wetting characteristics of SnAg: SnCu, SnAgBi, and SnAgCu lead-free solders on copper substrates, Journal of Electronic Materials 35 (7) (2006) 1530–1536.
[10] R.W. Snyder, Diffuse reflectance FT-IR analysis of rosin flux–metal oxide interactions, Applied Spectroscopy 41 (3) (1987) 460–463.
[11] L.J. Turbini, J.A. Jachim, G.B. Freeman, J.F. Lane, Characterizing water soluble fluxes: surface insulation resistance vs electrochemical migration, in: Electronics Manufacturing Technology Symposium. Thirteenth IEEE/CHMT International, 1992, pp. 80–84.
[12] T. Hetschel, K.J. Wolter, F. Phillipp, Wettability effects of immersion tin final finishes with lead free solder, in: Electronics System-Integration Technology Conference, 2008. ESTC, 2nd, 2008, pp. 561–566.
[13] S.C. Britton, J.C. Sherlock, Examination of oxides on tin surfaces by cathodic reduction, British Corrosion Journal 9 (1974) 96–102.
[14] U. Ray, I. Artaki, H.M. Gordon, P.T. Vianco, The influence of temperature and humidity on printed wiring board surface finishes: immersion tin vs organic azoles, Journal of Electronics Materials 23 (1994) 779–785.
[15] A. Kolmakov, Y. Zhang, M. Moskovits, Topotactic thermal oxidation of Sn nanowires: intermediate suboxides and core–shell metastable structures, Nano Letters 3 (8) (2003) 1125–1129.
[16] C.H. Shek, J.K.L. Lai, G.M. Lin, Y.F. Zheng, W.H. Liu, Nanomicrostructure: chemical stability and abnormal transformation in ultrafine particles of oxidized tin, Journal of Physics and Chemistry of Solids 58 (1) (1997) 13–17.
[17] X. Sun, S. Ju, D. Janes, B. Yu, Self-assembly of low-dimensional phase-change nanomaterials for information storage, in: Nanotechnology, 2007. IEEE-NANO. 7th IEEE Conference, 2007, pp. 1067–1071.
[18] F. Gao, Z. Gu, Nano-soldering of magnetically aligned three-dimensional nanowire networks, Nanotechnology 21 (11) (2010) 115604.
[19] A. Rai, D. Lee, K. Park, M.R. Zachariah, Importance of phase change of aluminum in oxidation of aluminum nanoparticles, The Journal of Physical Chemistry B 108 (39) (2004) 14793–14795.
[20] S. Mukherjee, X. Li, F. Gao, Z. Gu, An efficient silver etchant for the fabrication of active nanowires using anodized aluminum oxide templates, Electrochemical and Solid-State Letters 13 (7) (2010) D50–D52.
[21] D.-X. Xu, Y.-P. Lei, Z.-D. Xia, F. Guo, Y.-W. Shi, Experimental wettability study of lead-free solder on cu substrates using varying flux and temperature, Journal of Electronic Materials 37 (1) (2008) 125–133.
[22] A. Safaei, M.A. Shandiz, S. Sanjabi, Z.H. Barber, Modelling the size effect on the melting temperature of nanoparticles, nanowires and nanofilms, Journal of Physics: Condensed Matter 19 (2007) 2162161–2162169.
[23] S.S. Dalgic, U. Domekeli, Melting properties of tin nanoparticles by molecular dynamics simulation, Journal of Optoelectronics and Advanced Materials 11 (12) (2009) 2126–2132.
[24] T. Bachels, H.-J. Güntherodt, R. Schäfer, Melting of isolated tin nanoparticles, Physical Review Letters 85 (6) (2000) 1250–1253.
[25] C.D. Zou, Y.L. Gao, B. Yang, X.Z. Xia, Q.J. Zhai, C. Andersson, J. Liu, Nanoparticles of the lead-free solder alloy Sn–3.0Ag–0.5Cu with large melting temperature depression, Journal of Electronic Materials 38 (2) (2009) 351–355.
[26] P. Song, D. Wen, Experimental investigation of the oxidation of tin nanoparticles, The Journal of Physical Chemistry C 113 (31) (2009) 13470–13476.
[27] P.M. Ajayan, L.D. Marks, Quasimelting and phases of small particles, Physical Review Letters 60 (7) (1988) 585–587.
[28] P.M. Ajayan, L.D. Marks, Experimental evidence for quasimelting in small particles, Physical Review Letters 63 (3) (1989) 279–282.
[29] S. Iijima, P.M. Ajayan, Substrate and size effects on the coalescence of small particles, Journal of Applied Physics 70 (9) (1991) 5138–5140.
[30] G.S. Wable, S. Chada, B. Neal, R.A. Fournelle, Solidification shrinkage defects in electronic solders, JOM 57 (6) (2005) 38–42.